Low Temperature Physics/Fizika Nizkikh Temperatur, 2019, v. 45, No. 9, pp. 1208–1216

Coulomb effects on thermally induced shuttling of spin-polarized electrons

O.A. Ilinskaya[1], A.D. Shkop[1], D. Radic[2], H.C. Park[3], I.V. Krive[1,4], R.I. Shekhter[5], and M. Jonson[5]

[1]*B. Verkin Institute for Low Temperature Physics and Engineering of the National Academy of Sciences of Ukraine, 47 Nauki Ave., Kharkiv 61103, Ukraine*
E-mail: ilinskaya@ilt.kharkov.ua

[2]*Department of Physics, Faculty of Science, University of Zagreb, Bijenicka 32, Zagreb 10000, Croatia*

[3]*Center for Theoretical Physics of Complex Systems, Institute for Basic Science (IBS), Daejeon 34051, Republic of Korea*
E-mail: hcpark@ibs.re.kr

[4]*Physical Department, V.N. Karazin Kharkiv National University, Kharkiv 61022, Ukraine*

[5]*Department of Physics, University of Gothenburg, SE-412 96 Göteborg, Sweden*

Received March 25, 2019, published online July 26, 2019

A thermally driven single-electron transistor with magnetic leads and a movable central island (a quantum dot) subject to an external magnetic field is considered. The possibility of a mechanical instability caused by magnetic exchange interactions between spin-polarized electrons in this system was studied by the density matrix method. We proved analytically that for noninteracting electrons in the dot there is no such mechanical instability. However, for finite strengths of the Coulomb correlations in the dot we numerically found critical magnetic fields separating regimes of mechanical instability and electron shuttling on the one hand and damped mechanical oscillations on the other. It was shown that thermally induced magnetic shuttling of spin-polarized electrons is a threshold phenomenon, and the dependence of the threshold bias temperature on model parameters was calculated.

Keywords: thermally driven single-electron shuttle, magnetic exchange interaction, spin-polarized electrons.

1. Introduction

Single-electron shuttling is a nonlinear, nonequilibrium, and temporally nonlocal nanoelectromechanical phenomenon first predicted in Refs. 1 and 2. Intriguingly, the simple classical oscillation of a charged particle between the plates of a voltage-biased capacitor (electric pendulum) acquires new features in the mesoscopic regime, which lead to novel physical effects. The interplay between electron tunneling, Coulomb blockade of tunneling and retardation effects on the mechanical oscillations of a movable quantum dot (QD), placed between voltage-biased leads of a mesoscopic transistor, yields a mechanical instability resulting in QD oscillations. This leads to a strong (exponential) increase of the electric current through the mesoscopic device, which can significantly contribute to new functionalities of molecular transistors [2] (see also the review [3]). There are various experiments, dealing with shuttle-like electron devices (see, e.g., Refs. 4 and 5).

An electric field, produced by a bias voltage acting on a QD charged from the source electrode, always attracts the dot to the drain electrode, thus providing a necessary condition for electron shuttling. If the dot is not pinned and dissipation in the mechanical subsystem is weak, electron shuttling always occurs when the (symmetrically applied) bias voltage exceeds a threshold value [2], $V > V_{\rm th} = (2/e)(\delta\varepsilon + \hbar\omega)$, where $\delta\varepsilon = \varepsilon_0 - \varepsilon_F$ is the energy of the single QD electron level measured from the Fermi energy of electrons in the leads, ε_F, ω is the angular frequency of dot oscillations, and $-e$ is electron charge. In the shuttle regime of electron transport the amplitude of dot oscillations saturates (limiting cycle) at a certain value $\mathcal{A}_m \geq \lambda$ (where λ is the characteristic tunneling length) due to the specific nonlinear and nonlocal in time dynamics of the mechanical subsys-

tem. Formally, saturation is explained by the fact that the calculated positive (when shuttling occurs) work done by the electric field during a closed dot trajectory stops to grow when the oscillation amplitude reaches its saturation value and both tunneling charging and discharging of the QD are strongly enhanced. (Note that the charge of the QD is changed due to electron tunneling to and from the dot.) A specific feature of the shuttling regime (periodic dot oscillations) of electron transport in single-electron transistors (SET) is a strong suppression of low-frequency noise compared with the shot noise, measured in a standard SET [6].

In a single-electron transistor with magnetic leads (see, e.g., Ref. 7, where a fullerene-based transistor with nickel leads was studied) electric shuttling of spin-polarized electrons can be controlled by an external magnetic field thus making the SET a new spintronic device [8]. In Ref. 9 a new mechanism of shuttling of spin-polarized electrons was suggested. It is based on the assumption that (magnetic) exchange forces, produced by the interaction of the electron spin in the dot with the magnetization in the leads, is larger than the electric force in a voltage-biased device. This assumption is supported by experiments such as Ref. 7, where the exchange field experienced by an electron spin in the dot was observed to be (in energy units) of the order of 10 meV. Spin accumulation in the QD at zero temperature appears due to tunneling of a spin-polarized electron from the source electrode. The exchange interaction between the magnetic moment associated with this spin and the magnetization of the leads gives rise to an exchange force that attracts the dot to the source and repels it from the drain. The exchange interaction itself can therefore not result in a magnetic shuttle current. In what follows we will consider fully and oppositely polarized leads (spin-up polarization in the source electrode and spin-down polarization in the drain electrode). To get electron transfer in this situation one has to introduce an external magnetic field H (oriented perpendicular to the magnetization in the leads), which induces spin precession and opens up for a current to flow. This is because a QD occupied by a spin-down electron is attracted to the drain electrode thus making magnetic shuttling possible. For the case when there is a Coulomb blockade of tunneling magnetic shuttling was indeed proven to exist at low magnetic fields [9].

Thermally induced magnetic shuttling, where the energy source for shuttling is a temperature difference between the leads (while their chemical potentials are the same), was considered in Ref. 10. It was shown there that, despite the presence of temperature-induced dissipation, in the Coulomb blockade regime the phenomenon of magnetic shuttling occurs at high temperature difference $\delta T \gg \Gamma$ (Γ is the dot level width [tunnel coupling energy] as determined by the rate of tunneling between dot and leads) in a finite region of magnetic fields $H_{c1} < H < H_{c2}$.

The aim of the present paper is to develop a theory of the magnetic shuttle [9,10] for the case of a finite Coulomb correlation energy U. We analytically solve the mechanical-stability problem for our system and show that for noninteracting electrons, $U = 0$, magnetic shuttling is not realized. For a voltage-biased magnetic device, the time evolution of mechanical quantum dot oscillations for different bias voltages is numerically studied. For a thermally biased device, the critical value $U = U_c$, when the shuttling phenomenon becomes possible, is calculated numerically using analytically derived equations for the magnetic shuttle dynamics. Our main result here is the dependence of an upper and a lower critical magnetic field on the strength of the Coulomb correlations U. These critical fields separate a regime where an initial fluctuation in the position of the QD develops into QD shuttling and a regime where such a fluctuation is damped out. It is shown also that thermo-induced shuttling is a threshold phenomenon and that the threshold value of the temperature difference found numerically is of the order of the sum of the level detuning $\delta\varepsilon = \varepsilon_0 - \varepsilon_F$ and the energy $\hbar\omega$ of the vibron quantum.

2. Hamiltonian and kinetic equations

We consider a movable quantum dot, placed in the middle of the gap between the leads of spin-polarized electrons (for equal chemical potentials in the leads our model is sketched in Fig. 1). The Hamiltonian of our system is a sum of three different terms, $\hat{H} = \hat{H}_l + \hat{H}_d + \hat{H}_t$. The leads of noninteracting spin-polarized electrons (we assume full

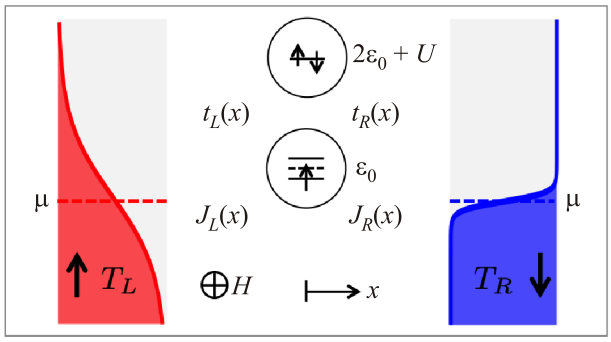

Fig. 1. (Color online) Schematic picture of a thermally driven magnetic shuttle. The leads, fully magnetized in opposite directions, are kept at equal chemical potentials $\mu \simeq \varepsilon_F$ but at different temperatures $T_L > T_R$. A movable quantum dot with a single-electron energy level, ε_0, spin-split by an external magnetic field H and magnetic exchange interactions with the leads, is coupled to the leads by electron tunneling [$t_{L/R}(x)$ and $J_{L/R}(x)$ are position-dependent tunneling amplitudes and exchange energies]. The external magnetic field, directed perpendicular to the magnetization in the leads, induces spin flips between spin-up and spin-down electron dot states, thus enabling an electron current. The energy of the doubly occupied dot is $2\varepsilon_0 + U$, where U is the Coulomb correlation energy.

polarization and consider opposite magnetization of the leads; we choose that electrons in the source, L-electrode, are spin-up polarized and in the drain, R-electrode, are spin-down polarized) are described by the Hamiltonian

$$\hat{H}_l = \sum_{k,j} \varepsilon_{k,j} a^\dagger_{k,j} a_{k,j}, \qquad j = L,R = \uparrow,\downarrow, \tag{1}$$

where $a^\dagger_{k,j}$ ($a_{k,j}$) is the creation (annihilation) operator with the momentum k ($\varepsilon_{k,j}$ is the electron energy) in the lead $j = L,R$.

The Hamiltonian of the quantum dot (QD) is a sum of two contributions, $\hat{H}_d = \hat{H}^e_d + \hat{H}^v_d$, describing, respectively, the interacting-electrons and vibron subsystems in the QD. We will model the vibronic subsystem by the Hamiltonian, $\hat{H}^v_d$, of a harmonic oscillator

$$\hat{H}^v_d = \frac{\hat{p}^2}{2m} + \frac{m\omega^2}{2}\hat{x}^2. \tag{2}$$

Here $\hat{x}$ and $\hat{p}$ are the center-of-mass coordinate and the corresponding momentum of the QD, m is the mass of the QD and ω is the angular frequency of the dot vibrations. The electronic part, $\hat{H}^e_d$, reads

$$\hat{H}^e_d = \sum_\sigma \varepsilon_\sigma(\hat{x}) c^\dagger_\sigma c_\sigma - \Omega_H \left(c^\dagger_\uparrow c_\downarrow + c^\dagger_\downarrow c_\uparrow \right) + U c^\dagger_\uparrow c_\uparrow c^\dagger_\downarrow c_\downarrow, \tag{3}$$

where $\varepsilon_\sigma(\hat{x}) = \varepsilon_0 - (\sigma/2)J(\hat{x})$ [with $\sigma = \uparrow, \downarrow = +, -$] is the spin- and position-dependent energy of the Zeeman split dot level ε_0 in the exchange field $J(\hat{x}) = J_L(\hat{x}) - J_R(\hat{x})$ (here $J_{L/R}(\hat{x}) = J_{L/R}\exp(\mp\hat{x}/\lambda_J)$ is the exchange energy per unit spin between ferromagnetic leads, L, R, and the spin on the dot, and λ_J is the characteristic decay length of the exchange interaction). In Eq. (3) $\Omega_H/\hbar = g\mu_B H/(2\hbar)$ is the Larmor frequency of electron precession in the external magnetic field H, directed perpendicular to the antiparallel magnetization in the leads, g is the gyromagnetic ratio, μ_B is the Bohr magneton; U is the Coulomb repulsion energy. Notice that coordinate dependence of energy $\varepsilon_\sigma(\hat{x})$ introduces an electron-vibron interaction in our model. This interaction appears also in the tunneling Hamiltonian

$$\hat{H}_t = t_L(\hat{x}) \sum_k c^\dagger_\uparrow a_{k,L} + t_R(\hat{x}) \sum_k c^\dagger_\downarrow a_{k,R} + \text{h.c.}, \tag{4}$$

when one takes into account the coordinate dependence of the tunneling amplitudes, $t_{L,R}(\hat{x})$. We will model this $\hat{x}$-dependence by the one-parameter exponential function $t_{L/R}(\hat{x}) = \exp(\mp\hat{x}/2\lambda)$, where λ is the characteristic tunneling length, and the dot coordinate, $\hat{x}$, is measured from the isolated dot position. In what follows we will consider $\hat{x}$ and $\hat{p}$ (see Eq. (2)) as classical variables and assume that the equilibrium position of the isolated dot corresponds to $x = 0$.

In this section our aim is to derive an equation of motion for the dot center-of-mass coordinate $x(t)$. We solve this nonlinear and nonlocal in time problem to lowest order in the dot tunneling coupling energy Γ_j, namely, $\Gamma_j \ll \max\{T_j, eV\}$ (here $\Gamma_j = 2\pi\nu_F |t_j|^2$, $j = L,R$, ν_F is the density of states at the Fermi energy, $eV = \mu_L - \mu_R$, and $T_{L,R}$ and $\mu_{L,R}$ are the temperatures and chemical potentials of the leads described by the Fermi distribution function). We use the density operator method to solve the problem. For conditions outlined above, which physically imply sequential electron tunneling through the dot, the density operator $\hat{\rho}$ can be represented as a product of the equilibrium density matrix of the leads and the QD density operator $\hat{\rho}_d$. Then all electronic degrees of freedom in the leads can be averaged out in the Liouville–von Neumann equation for density operator. The relevant Fock space is spanned by four electron states. These are the ground state (empty QD) $|0\rangle$, the states corresponding to a QD singly occupied by a spin-up (spin-down) electron, $|\uparrow(\downarrow)\rangle = c^\dagger_{\uparrow(\downarrow)}|0\rangle$, and the doubly occupied electron state, $|2\rangle = c^\dagger_\uparrow c^\dagger_\downarrow |0\rangle$. In this space the matrix elements of $\hat{\rho}_d$ form a 6-vector with components $\rho_0 = \langle 0|\hat{\rho}_d|0\rangle$, $\rho_\uparrow = \langle\uparrow|\hat{\rho}_d|\uparrow\rangle$, $\rho_\downarrow = \langle\downarrow|\hat{\rho}_d|\downarrow\rangle$, $\rho_{\uparrow\downarrow} = \langle\uparrow|\hat{\rho}_d|\downarrow\rangle = \rho^*_{\downarrow\uparrow}$, $\rho_2 = \langle 2|\hat{\rho}_d|2\rangle$. The diagonal components of the density operator satisfy the normalization condition $\rho_0 + \rho_\uparrow + \rho_\downarrow + \rho_2 = 1$.

Following the procedure, worked out in detail in Refs. 8 and 10, it is straightforward to derive a set of linear differential equations (see Appendix) for the elements of the density matrix (perturbation theory with respect to the tunneling level width allows one to make the kinetic equations local in time). The mechanical equation for $x(t)$ in terms of the QD population probabilities (ρ_j) is readily derived from the Hamiltonian (2), (3)

$$\frac{d^2x}{dt^2} + \omega^2 x = -\frac{1}{m}\text{Tr}\left\{\hat{\rho}_d \frac{\partial \hat{H}_d}{\partial x}\right\} = -\frac{1}{2m}\frac{\partial J(x)}{\partial x}\left(\rho_\uparrow - \rho_\downarrow\right). \tag{5}$$

Equations (A.1)–(A.5) (see Appendix) and Eq. (5) form a closed set of equations for our problem. They are used for numerical simulations of the position of the dot center-of-mass coordinate $x = x(t)$.

Note that only the difference of the spin-up and spin-down dot populations enters the r.h.s. of the mechanical equation of motion, Eq. (5). In what follows we will call this linear combination of probabilities the mechanically "active" one. This allows us to reduce by one the number of independent kinetic equations by considering the linear combinations of ρ_j. It is easy to show that the symmetric spin-neutral quantities $R_0 = \rho_0 + \rho_2$ and $\rho_\uparrow + \rho_\downarrow = 1 - R_0$ are decoupled from the equations for the four other linear combinations:

$$\begin{aligned} R_1 &= \rho_0 - \rho_2, \qquad R_2 = \rho_\uparrow - \rho_\downarrow, \\ R_3 &= -i(\rho_{\uparrow\downarrow} - \rho^*_{\uparrow\downarrow}), \quad R_4 = \rho_{\uparrow\downarrow} + \rho^*_{\uparrow\downarrow}. \end{aligned} \tag{6}$$

The system of equations for R_j, $j=1-4$, written in vector form, reads ($\hbar=1$)

$$|\dot{R}(t)\rangle = \hat{A}\{x(t),U\}\,|R(t)\rangle + |B\{x(t),U\}\rangle, \tag{7}$$

with $\hat{A}\{x(t),U\} = \hat{A}_\Gamma\{x(t),U\} + \hat{A}_H\{x(t),U\} + \hat{A}_J\{x(t),U\}$. Here we introduced matrices related to tunneling (subindex Γ), external magnetic field (subindex H) and exchange interaction (subindex J). They are represented in the following form:

$$\hat{A}_\Gamma\{x(t),U\} = -\frac{1}{2}\begin{pmatrix} F_+^{+,-} & -F_-^{-,+} & 0 & 0 \\ -F_-^{+,-} & F_+^{-,+} & 0 & 0 \\ 0 & 0 & F_+^{-,+} & 0 \\ 0 & 0 & 0 & F_+^{-,+} \end{pmatrix}, \tag{8}$$

$$\hat{A}_H\{x(t),U\} = \begin{pmatrix} 0 & 0 & 0 & -H_+^- \\ 0 & 0 & 2\Omega_H & H_-^- \\ 0 & -2\Omega_H & 0 & 0 \\ H_+^- & H_-^- & 0 & 0 \end{pmatrix}, \tag{9}$$

$$\hat{A}_J\{x(t),U\} = \frac{1}{2}\begin{pmatrix} -J_-^- & -J_+^- & 0 & 0 \\ J_+^- & J_-^- & 0 & 0 \\ 0 & 0 & -J_-^- & J(x) \\ 0 & 0 & -J(x) & J_-^- \end{pmatrix}. \tag{10}$$

In Eq. (7) the vector **B** (which appears when we use the normalization condition, $\mathrm{Tr}\,\hat{\rho}_d = 1$, to reduce the number of independent variables) takes the form

$$|B\{x(t)\}\rangle = \frac{1}{2}\begin{pmatrix} F_+^{-,-} - J_-^+ \\ -F_-^{-,-} + J_+^+ \\ 0 \\ 2H_+^+ \end{pmatrix}. \tag{11}$$

Here the quantities $F_\pm^{j,k}$, where $j,k=(+,-)$, $H_\pm^\eta$ and $J_\pm^\eta$ (here $\eta=\pm1$) depend on the tunneling coupling energies $\Gamma_{L,R}[x(t)]$ and the Fermi distribution functions $f_{L,R}(\varepsilon)$ and $f_{L,R}(\varepsilon+U)$,

$$F_\pm^{j,k} = \Gamma_\pm(x) + j\left[\Gamma_L(x) f_L^+ \pm \Gamma_R(x) f_R^+\right] + k\left[\Gamma_L(x) f_L^{U,+} \pm \Gamma_R(x) f_R^{U,+}\right], \tag{12}$$

$$H_\pm^\eta = \left\{\Gamma_L(x) f_L^- \pm \Gamma_R(x) f_R^- + \eta\left[\Gamma_L(x) f_L^{U,-} \pm \Gamma_R(x) f_R^{U,-}\right]\right\}\Omega_H \Big/ \sqrt{4\Omega_H^2 + J^2(x)}, \tag{13}$$

$$J_\pm^\eta = H_\pm^\eta J(x)/\Omega_H. \tag{14}$$

In Eqs. (12)–(14) the following notation is introduced: $\Gamma_\pm(x) = \Gamma_L(x) \pm \Gamma_R(x)$, $2f_{L,R}^\pm = f_{L,R}(E_-) \pm f_{L,R}(E_+)$ and $2f_{L,R}^{U,\pm} = f_{L,R}(E_-+U) \pm f_{L,R}(E_++U)$. Here $f_j(\varepsilon) = \{1+\exp[(\varepsilon-\mu_j)/T_j]\}^{-1}$ is the Fermi distribution function in $j=L,R$ electrode, and

$$E_\pm = \varepsilon_0 \pm \frac{\sqrt{J^2(x)+4\Omega_H^2}}{2}. \tag{15}$$

To proceed further with analytical calculations we analyze the onset of instability, when the displacement $x(t)$ is small (but much larger than the amplitude of the zero-point fluctuations $x_0 \simeq \sqrt{\hbar/(m\omega)}$ so that our classical description of the vibronic subsystem is justified).

We solve the equation system (7) by expanding $R_i(t)$ to linear order in the displacement x, which is assumed to be small. Hence, $R_i(t) \approx R_i^0 + R_i^1(t)$, where $R_i^1(t) \propto x(t)$. At first we consider noninteracting electrons, $U=0$, and a symmetric junction, $\Gamma_L(x=0) = \Gamma_R(x=0) = \Gamma$, $J_L(x=0) = J_R(x=0) = J$. Then the equations for R_1^1 and R_4^1 are decoupled from the equations for R_2^1 and R_3^1. Therefore the analysis of the mechanical instability in this particular case is reduced to a simple problem — one has to solve two coupled linear equations,

$$\begin{pmatrix} \dot{R}_2^1 \\ \dot{R}_3^1 \end{pmatrix} = \begin{pmatrix} -\Gamma & 2\Omega_H \\ -2\Omega_H & -\Gamma \end{pmatrix}\begin{pmatrix} R_2^1 \\ R_3^1 \end{pmatrix} - \alpha(f_L^- + f_R^-)\begin{pmatrix} \Gamma/(2\Omega_H) \\ 1 \end{pmatrix} x(t), \tag{16}$$

where $\alpha > 0$ (the exchange force) is minus the derivative of the exchange energy, $J(x) \approx -\alpha x$. Substituting the solution R_2^1 into Eq. (5), we obtain the rate of change, r, of the amplitude of nanomechanical vibrations $x(t) \propto \exp(i\Omega t)$ at $U=0$:

$$r = -\mathrm{Im}\Omega = -\frac{\hbar\alpha^2}{16m}\sum_{j=L,R}\frac{f_j(\varepsilon_0-\Omega_H) - f_j(\varepsilon_0+\Omega_H)}{\Omega_H} \times \frac{\Gamma[\Gamma^2 + (\hbar\omega)^2 + 4\Omega_H^2]}{[\Gamma^2 - (\hbar\omega)^2 + 4\Omega_H^2]^2 + 4(\hbar\omega)^2\Gamma^2}. \tag{17}$$

Since the Fermi distribution function $f_j(\varepsilon)$ is a decreasing function of energy ($\varepsilon > 0$) and $\Omega_H \geq 0$ by definition, $r(H)$ is always negative for $H \neq 0$. This means that for noninteracting electrons ($U=0$) there is no mechanical instability for the considered magnetic device. On the other hand, in Ref. 10 (see also Ref. 9) it was analytically proven that in the regime of Coulomb blockade (formally $U \to \infty$ and therefore $\rho_2 = 0$) the shuttling regime of electron transport is realized at low magnetic fields $\Omega_H < (\sqrt{7}/2)\sqrt{\Gamma^2 + (\hbar\omega)^2}$. This

means that for finite U there is a critical value, $U = U_c$, when there is a crossover from the shuttling regime to a regime where mechanical dot fluctuations are damped out. Notice that in the limit $\Omega_H \to 0$ Eq. (17) is transformed to the magnetic friction coefficient

$$r_J(T) \simeq -\frac{\hbar\alpha^2}{m}\frac{\Gamma}{\Gamma^2+(\hbar\omega)^2}\frac{1}{T}\cosh^{-2}\left(\frac{\varepsilon_0-\varepsilon_F}{2T}\right), \quad (18)$$

first introduced in Ref. 10, where T is the temperature of the left lead, and the temperature of the right lead equals zero.

In other words Coulomb correlations promote electron shuttling in a magnetic nanomechanical device, Ref. 11. The dependence of the critical Coulomb energy on temperature and other model parameters was studied in detail in Ref. 11.

3. Influence of electron-electron correlations on electron shuttling in a voltage-biased magnetic device

In this section we consider the influence of Coulomb correlations on the instability of mechanical vibrations in a voltage-biased magnetic device. In our model, Eqs. (1)–(4), we neglect electric forces, acting on electrons in the QD, compared with magnetic forces. In experiments on a C_{60}-based molecular transistor [7] the exchange interaction between the electron spin on the fullerene and magnetic (Ni) leads was shown to be strong (of the order of 10 meV). The electric field, acting on a charged molecule, strongly depends on the device geometry but can be roughly estimated to be $E \sim V/d$, where d is the distance between the leads. In what follows, when studying the influence of electron-electron interaction on the functionality of magnetic shuttle, we will assume that the exchange force $\sim J/\lambda_J$ exceeds the electric force. Indeed, we estimated that the maximum ratio of electric force to exchange force for bias voltages from Fig. 2 (see below) is about 0.3, therefore electric forces can be neglected. In this case the bias voltage plays the role of an energy supply for a purely magnetic device, controlled by the external magnetic field H. We will also assume a large temperature difference ($T_L \gg T_R$) in our device. This situation favors the shuttling regime, by providing an extra energy supply, and by suppressing temperature-induced dissipation in the drain (right lead), as well as facilitating electron tunneling to empty states in the right electrode.

To analyze the fully developed shuttle vibrations one has to deal with the nonlinear and nonlocal spintromechanics numerically. In Fig. 2 we present results of numerical simulations for the case of a symmetric junction, solving the system of equations for the components of the density matrix [Eqs. (A.1)–(A.5) in the Appendix], coupled to the mechanical equation of motion, Eq. (5). The eight panels in the figure show the time evolution for different bias voltages of the amplitude $\mathcal{A}(t)$ of the mechanical QD oscillations after an initial spontaneous fluctuation of the QD position. The evolution is shown on a time scale more

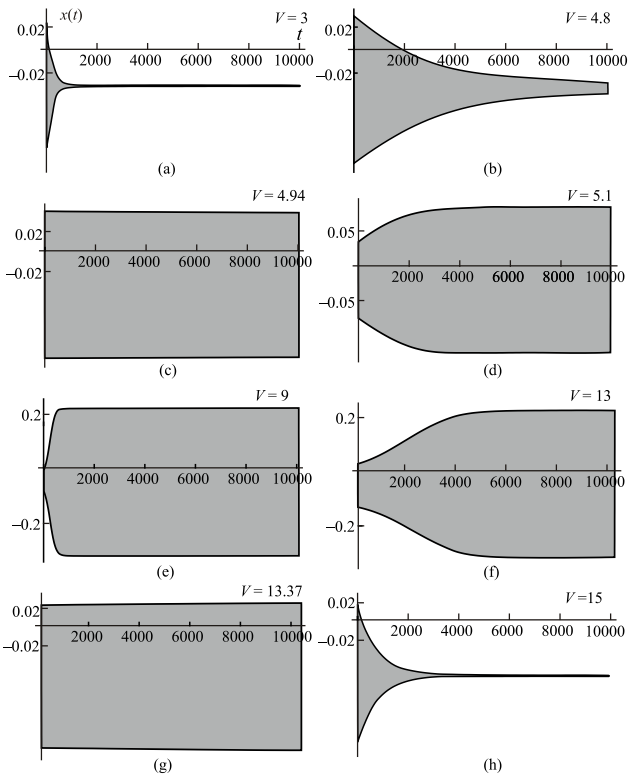

Fig. 2. Time evolution of mechanical QD oscillations after an initial spontaneous fluctuation in QD position plotted for different bias voltages. The upper and lower borders of the dark areas form the envelope of the (unresolved) oscillations, whose amplitude $\mathcal{A}(t)$ is half the vertical distance between these borders. The mechanical displacement is scaled to the characteristic tunneling length λ and time to $\hbar/\Gamma$. All energies are scaled to Γ_L, in particular, the bias voltage parameter $eV/\Gamma_L \to V$. Parameters, used in simulations, are the following: temperature $T/\Gamma_L = 1$, mechanical frequency $\hbar\omega/\Gamma_L = 1$, magnetic field energy $\Omega_H/\Gamma_L = 0.7$, exchange energy $J/\Gamma_L = 1.5$, level detuning energy $\delta\varepsilon/\Gamma_L = 2$ and the Coulomb correlation energy $U/\Gamma_L = 10$. Junction is considered symmetrical ($\Gamma_L = \Gamma_R$) and tunneling length is equal to the exchange length ($\lambda = \lambda_J$), dimensionless electromechanical coupling constant, entering the r.h.s. of mechanical equation, written in dimensionless variables, $\kappa = \hbar^2 J/(m\lambda\lambda_J\Gamma_L^2) = 0.09$. In plots (a)–(d) we see the onset of the instability, taking place for $V = 4.94$. The instability is well developed on the interval $V \in (4.94, 13.37)$ [plots (e)–(f)]. At critical value of bias voltage $V_c = 13.37$ the instability deteriorates and the system becomes stable for larger values of V [plots (g)–(h)].

than three orders of magnitude longer than the oscillation period. At low temperatures $T \ll \Gamma, \delta\varepsilon$ the influence of the electron subsystem on the mechanical vibrations occurs only when the bias voltage exceeds the energy E_-, see Eq. (15), of a spin-up electron on the dot. As was shown earlier [2], the shuttling regime of electron transport at $T_{L,R} = 0$ is realized for a non-symmetrically applied bias voltage V when $eV > eV_{\text{th}} = \delta\varepsilon + \hbar\omega$. The plots in Figs. 2(a)–(d) demonstrate the onset and time development

of electron shuttling in our magnetic device. We see that the critical voltage [plot (c)], determined for the case of a finite temperature $T_L = \Gamma$ of the source lead, is close to the above theoretical value. In this section we focus on the spintromechanically interesting regime of electron transport when $V > V_{\text{th}}$. Then single occupation of the dot level is possible due to electron tunneling from the source electrode, and double occupation at zero temperature may occur only at energies exceeding the excitation energy of the doubly occupied electron state $\mu_L > U + \varepsilon_0$. If the bias voltage is such that μ_L is close to but still lower than this value (see Fig. 1) double occupation occurs as a result of thermal fluctuations, which allows temperature to control the influence of the Coulomb blockade phenomenon on the nanomechanics.

Doubly occupied QD electron states, having zero total spin, do not interact with the exchange field and can therefore not contribute to electron shuttling. By increasing the population of these states (by increasing the temperature), a transition from the shuttling regime of oscillations to the regime of damped mechanical oscillations occurs at a certain (critical) value of the ratio $\rho_2/\rho_\downarrow = n_c$. One can roughly estimate this quantity when the activation energy of the two-electron state $U^* = \varepsilon_0 + U - \mu_L \gg T_L = T$. We assume that under certain conditions (see below) only the two quantities ρ_2 and $\rho_\downarrow$ determine the mechanical behavior in the critical region. The two coupled linear equations for these probabilities are readily derived from Eqs. (A.5), (A.3) in the limit $\Omega_H \to 0$. In the steady state regime ($\dot{\rho}_j = 0$) and for $f_R = 0$, $f_L(U) \simeq \exp(-U^*/T) \ll 1$, the equations take the simple form

$$[\Gamma_L(a_m) + \Gamma_R(a_m)]\rho_2 = \Gamma_L(a_m) f_L(U)\rho_\downarrow,$$

$$\Gamma_L(a_m)\rho_2 = \Gamma_R(a_m)\rho_\downarrow. \qquad (19)$$

Here a_m is the dimensionless amplitude (measured in units of the tunneling length λ) of developed shuttle oscillations at the dot position, most favorable for electron tunneling from the source electrode to the $|\downarrow\rangle$-state (this process populates the mechanically inactive doubly occupied state, which in the critical region stops the shuttling). A nontrivial solution of Eq. (19) exists when $\Gamma_L(a_m)/\Gamma_R(a_m) = \Gamma_L/\Gamma_R \exp(2a_m) \gg 1$. It reads $n_c \simeq f_L(U) \simeq \Gamma_R(a_m)/\Gamma_L(a_m) \ll 1$. Therefore our simple analysis predicts a linear dependence of the critical value U_c^* on temperature for low temperatures and low magnetic fields,

$$U_c^* \simeq T\left[\ln\frac{\Gamma_L}{\Gamma_R} + 2a_m\right]. \qquad (20)$$

Numerical simulations are in agreement with this prediction (see Ref. 11).

A remarkable feature of the plots is that when a shuttle instability occurs the amplitude of mechanical oscillations saturates at a certain value despite the fact that we do not include any phenomenological mechanical friction in Eq. (5). The intrinsic magnetic friction, Eq. (18), is small in our system at temperatures $T \ll \delta\varepsilon$. This self-saturation is a specific property of the nonlinear dynamics of our magnetic shuttle [9] (see also Ref. 2).

4. Coulomb effects in a thermally driven magnetic shuttle

Now we set $\mu_L = \mu_R = \varepsilon_F$ and consider electron shuttling driven by the difference in the temperatures of the leads, $\delta T = T_L - T_R$. In Ref. 10 it was shown that in the Coulomb blockade regime ($U \to \infty$) thermally induced shuttling occurs in a finite range of magnetic fields $H_{c1} < H < H_{c2}$. The corresponding upper magnetic energy, Ω_H^{c2} at $\delta T \gg \Gamma$ (a symmetric junction was studied) saturates to the value $\Omega_H^{c2} = (\sqrt{7}/2)\sqrt{\Gamma^2 + (\hbar\omega)^2}$. The lower magnetic energy Ω_H^{c1} is determined by magnetic friction, Eq. (18). In Ref. 10 the lower magnetic energy was found to scale, for temperature $T \gg \Gamma$, as $H_{c1} \propto \sqrt{T}(\Gamma/T)$. The "window" δH_c, where thermally induced electron shuttling occurs, is of the order of H_{c2} (see Fig. 2 in Ref. 10) and in dimensionless quantities (normalized by Γ) this window is not large. Then the question arises — is there a possibility for thermally induced shuttling in the case when Coulomb blockade is not pronounced (finite U)? Analytic calculations, Eq. (17), showed that for noninteracting electrons ($U = 0$) at arbitrary temperatures in the leads electron shuttling is absent in our model. Therefore there is critical value of Coulomb correlation energy $U = U_c$ when shuttling is replaced by damping of mechanical vibrations.

To answer the question posed above we will numerically solve Eqs. (A.1)–(A.5). It is reasonable to consider a situation where the temperatures in both leads are finite and $T_L > T_R$; we also assume $T_L \gg \Gamma_L$ and $T_R \gg \Gamma_R$ (these inequalities are necessary to justify the perturbation approach, when $\mu_L = \mu_R$, for the derivation of the kinetic equations). We will study the dependence of the upper and lower critical magnetic fields at finite Coulomb correlation energy U on the temperature difference δT and on the average temperature $T = (T_L + T_R)/2$. The numerical approach developed in the previous section allows one to obtain the dependence of the critical magnetic fields, which separate "shuttling" and "vibronic" regions of mechanical oscillations, on different parameters of our model. Here we consider the dependence of the critical magnetic fields on the strength U of the Coulomb interaction, and on the temperatures of the leads.

In Fig. 3 the dependence of $\Omega_H^{c1,c2}$ on U for given δT and T is presented. It is clearly seen from the plot that in the regime of Coulomb blockade $U \gg T$ the shuttling for large values of δT occurs in a finite range of $\delta\Omega_H^c = \Omega_H^{c2} - \Omega_H^{c1}$ (numerically close to analytic values, predicted in Ref. 10 for $U \to \infty$). The window for shuttling weakly depends on U down to $U \simeq T$, when the Coulomb blockade is lifted

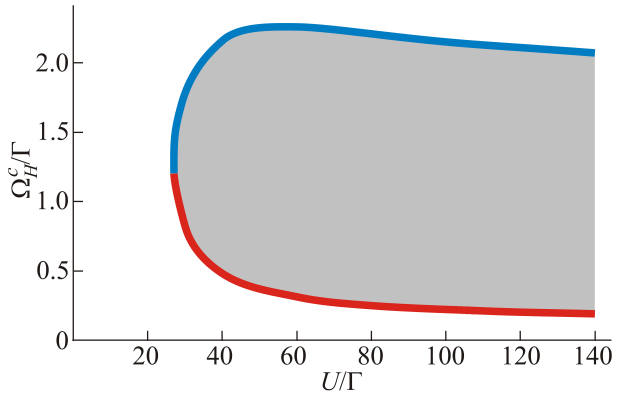

Fig. 3. (Color online) Dependence of the critical magnetic field Ω_H^c (measured in energy units, $\Omega_H = g\mu_B H/2$) on the Coulomb correlation energy U. The critical field separates shuttling (shaded) and damping regions of quantum dot oscillations. The upper critical field Ω_H^{c2} is plotted as a blue curve, the lower critical field Ω_H^{c1} — as a red curve. In the Coulomb blockade regime, $U \gg T_L$ ($T_L = 50\Gamma; T_R = 3\Gamma$), the window $\delta\Omega_H = \Omega_H^{c2} - \Omega_H^{c1}$ for shuttling is in agreement with analytical results [10]. At $U \simeq T_L$ the Coulomb blockade is lifted and $\delta\Omega_H$ shrinks to zero. A symmetric ($\Gamma_L = \Gamma_R = \Gamma$, $J_L = J_R = J$, $\lambda = \lambda_J$) and voltage unbiased junction is considered. We used the following parameters in the simulations: $J = 0.2\Gamma$, $\hbar\omega = 0.1\Gamma$, level detuning energy $\delta\varepsilon = 10\Gamma$.

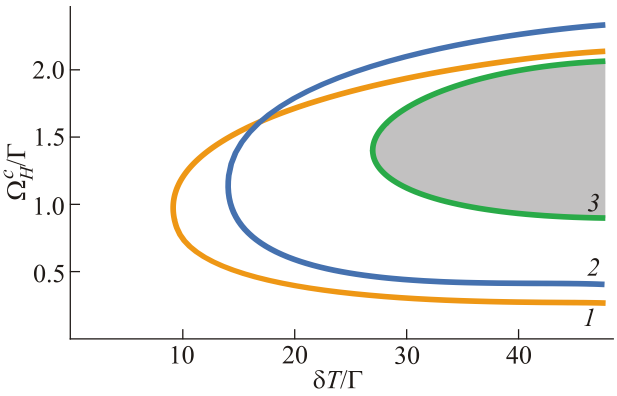

Fig. 4. (Color online) Dependence of the critical magnetic field (in energy units, $\Omega_H^c = g\mu_B H_c/2$) on the temperature difference between the leads, $\delta T = T_L - T_R$. The plots demonstrate the growth of the threshold value δT_{th} with the increase of the mechanical vibration frequency ω: curve *1* corresponds to $\hbar\omega = \Gamma$, curve *2* — $\hbar\omega = 3\Gamma$, curve *3* — $\hbar\omega = 5\Gamma$. The shuttle regime corresponds to the area between the lower and upper critical fields (shaded region for the case of $\hbar\omega = 5\Gamma$). The parameters used in simulations: $U = 100\Gamma$, $T_R = 3\Gamma$, $J = 1\Gamma$, $\delta\varepsilon = 10\Gamma$.

and $\delta\Omega_H^c$ shrinks to zero at some critical value of the ratio $\rho_2/\rho_\downarrow$, when temperature-induced mechanically inactive doubly populated electron states stop electron shuttling (see the discussion in the previous section).

Figure 4 demonstrates the behavior of the critical magnetic fields as a function of temperature differences δT for different values of the mechanical frequency ω. In Ref. 10, where analytic expressions for the critical magnetic fields were obtained, only the high-temperature limit $\delta T \to \infty$ was considered for $T_R = 0$. We see from the figure that temperature-induced electron shuttling is a threshold phenomenon. The threshold value δT_{th} strongly depends on level energy detuning $\delta\varepsilon$ (as it should be), mechanical frequency and average temperature T. It is well known [2] that for an electric shuttle (i.e., one driven by electric forces) at $T = 0$ the threshold bias voltage (if the bias is symmetrically applied) is $eV_{\text{th}}/2 = \delta\varepsilon + \hbar\omega$. The sharp onset of mechanical instability at this voltage occurs at temperatures $T \ll eV_{\text{th}}$. Finite temperatures smooth out the sharpness in the critical region. So it is not evident from a qualitative picture of the "shuttle instability" that the threshold δT_{th} for a magnetic shuttle is determined by the sum of detuning energy and vibron energy $\hbar\omega$. Numerical simulations, Fig. 4, show that the threshold δT does not satisfy (as it was expected) a simple formula such as that valid for the threshold bias voltage of an electric shuttle. However, numerically δT_{th} is still of the order of the sum of level detuning energy $\delta\varepsilon$ and vibron energy $\hbar\omega$. Our calculations show that the threshold temperature difference increases with the increase of $\delta\varepsilon$ (as it should be). More interesting is that δT_{th} grows when the mechanical frequency ω is increased (see Fig. 4).

The dependence of the threshold temperature difference on the average temperature T is illustrated in Fig. 5. It is clearly seen from the figure that the threshold δT for shuttling at "high temperatures" ($T > \delta\varepsilon$) depends on the average temperature. In this region $\delta T_{\text{th}} \gtrsim T$. At temperatures $T \ll \delta\varepsilon$ the threshold δT_{th} weakly depends on T (see the lower curve in Fig. 5 where δT_{th} is slightly smaller than

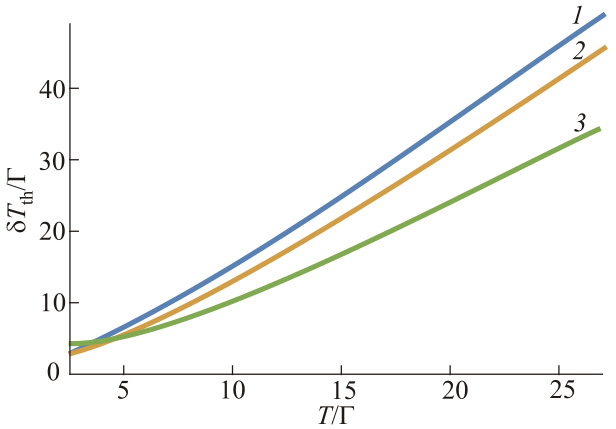

Fig. 5. (Color online) Dependence of the threshold temperature difference δT_{th} on the average temperature $T = (T_L + T_R)/2$ for different values of $\delta\varepsilon$: curve *1* corresponds to $\delta\varepsilon = 3\Gamma$, curve *2* — $\delta\varepsilon = 5\Gamma$, and curve *3* — $\delta\varepsilon = 10\Gamma$. The Coulomb blockade regime, $U = 300\Gamma \gg T$, is considered and $J = 0.3\Gamma$, $\hbar\omega = 0.2\Gamma$.

the average temperature). Notice that shuttling vanishes when the temperature in the drain ("R") lead exceeds $\delta\varepsilon$. In this case magnetic friction, Eq. (18), strongly impedes shuttling and a mechanical instability occurs only for very large values of δT.

5. Conclusion

The phenomenon of electron shuttling, first predicted for charge transport in mesoscopic transistors [1] (electric shuttle), was then considered for superconducting [12] (see also the review Ref. 13) and magnetic systems [8,9]. The fusion of electron spin dynamics with nanomechanics, called spintromechanics [14], allows one to control mechanical oscillations by electric and magnetic gates. Moreover, a mechanical subsystem, integrated into electrical and spintronic circuits, could be used not only for energy pumping into a system, but also for cooling of vibronic excitations, providing another road to quantum nanomechanics.

Voltage-biased junctions are more suitable for electric shuttling applications, since electron-number fluctuations in the dot do not have any detrimental effect on mechanical oscillations (shuttling). In contrast, electron number parity effects are significant for temperature-induced magnetic shuttling. In our paper it was shown that Coulomb effects, by suppressing electron number fluctuations, promote shuttling of spin-polarized electrons in temperature-biased junctions. This will lead to a strong enhancement of thermo-transport. We also demonstrated in the present paper, that thermally induced shuttling is a threshold phenomenon. This fact inevitably will result in mechanically-induced nonlinear effects in thermo-transport in a shuttle-based single-electron transistor.

Acknowledgment

This work was supported by the Institute for Basic Science in Korea (IBS-R024-D1); the National Academy of Sciences of Ukraine (grant No. 4/19-N and Scientific Program 1.4.10.26.4); the Croatian Science Foundation, project IP-2016-06-2289, and by the QuantiXLie Centre of Excellence, a project cofinanced by the Croatian Government and the European Union through the European Regional Development Fund — the Competitiveness and Cohesion Operational Programme (Grant KK.01.1.1.01.0004). The authors acknowledge the hospitality of PCS IBS in Daejeon (Korea).

Appendix A: The system of equations for matrix elements of dot density operator

The system of equations for the matrix elements of the dot density operator reads

$$\frac{\partial\rho_0}{\partial t}=\Gamma_L(x)(1-f_L^+)\rho_\uparrow+\Gamma_R(x)(1-f_R^+)\rho_\downarrow-\Gamma_L(x)f_L^+\rho_0-\Gamma_R(x)f_R^+\rho_0-$$

$$-\Upsilon_{1L}(x)(\rho_0+\rho_\uparrow)+\Upsilon_{1R}(x)(\rho_0+\rho_\downarrow)-(\Upsilon_{2L}(x)+\Upsilon_{2R}(x))(\rho_{\uparrow\downarrow}+\rho_{\uparrow\downarrow}^*); \tag{A.1}$$

$$\frac{\partial\rho_\uparrow}{\partial t}=-i\Omega_H(\rho_{\uparrow\downarrow}-\rho_{\uparrow\downarrow}^*)-\Gamma_L(x)(1-f_L^+)\rho_\uparrow+\Gamma_L(x)f_L^+\rho_0-\Gamma_R(x)f_R^{U,+}\rho_\uparrow+\Gamma_R(x)(1-f_R^{U,+})\rho_2+$$

$$+\Upsilon_{1L}(x)(\rho_0+\rho_\uparrow)+\Upsilon_{1R}^U(x)(\rho_\uparrow+\rho_2)+(\Upsilon_{2L}(x)+\Upsilon_{2R}^U(x))(\rho_{\uparrow\downarrow}+\rho_{\uparrow\downarrow}^*); \tag{A.2}$$

$$\frac{\partial\rho_\downarrow}{\partial t}=i\Omega_H(\rho_{\uparrow\downarrow}-\rho_{\uparrow\downarrow}^*)+\Gamma_L(x)(1-f_L^{U,+})\rho_2-\Gamma_L(x)f_L^{U,+}\rho_\downarrow-\Gamma_R(x)(1-f_R^+)\rho_\downarrow+\Gamma_R(x)f_R^+\rho_0-$$

$$-\Upsilon_{1L}^U(x)(\rho_\downarrow+\rho_2)-\Upsilon_{1R}(x)(\rho_0+\rho_\downarrow)+(\Upsilon_{2L}^U(x)+\Upsilon_{2R}(x))(\rho_{\uparrow\downarrow}+\rho_{\uparrow\downarrow}^*); \tag{A.3}$$

$$\frac{\partial\rho_{\uparrow\downarrow}}{\partial t}=-i\Omega_H(\rho_\uparrow-\rho_\downarrow)+iJ(x)\rho_{\uparrow\downarrow}-\frac{1}{2}\Gamma_L(x)(1-f_L^++f_L^{U,+})\rho_{\uparrow\downarrow}-\frac{1}{2}\Gamma_R(x)(1-f_R^++f_R^{U,+})\rho_{\uparrow\downarrow}-$$

$$-\frac{1}{2}(\Upsilon_{1L}(x)-\Upsilon_{1L}^U(x))\rho_{\uparrow\downarrow}+\frac{1}{2}(\Upsilon_{1R}(x)-\Upsilon_{1R}^U(x))\rho_{\uparrow\downarrow}+$$

$$+\Upsilon_{2L}(x)(\rho_0+\rho_\uparrow)+\Upsilon_{2L}^U(x)(\rho_\downarrow+\rho_2)+\Upsilon_{2R}(x)(\rho_0+\rho_\downarrow)+\Upsilon_{2R}^U(x)(\rho_\uparrow+\rho_2); \tag{A.4}$$

$$\frac{\partial\rho_2}{\partial t}=-\Gamma_L(x)(1-f_L^{U,+})\rho_2-\Gamma_R(x)(1-f_R^{U,+})\rho_2+\Gamma_L(x)f_L^{U,+}\rho_\downarrow+\Gamma_R(x)f_R^{U,+}\rho_\uparrow+$$

$$+\Upsilon_{1L}^U(x)(\rho_\downarrow+\rho_2)-\Upsilon_{1R}^U(x)(\rho_\uparrow+\rho_2)-(\Upsilon_{2L}^U(x)+\Upsilon_{2R}^U(x))(\rho_{\uparrow\downarrow}+\rho_{\uparrow\downarrow}^*), \tag{A.5}$$

where

$$\Upsilon_{1L/R}(x) = f^{-}_{L/R}\frac{J(x)\Gamma_{L/R}(x)}{\sqrt{J^2(x)+4\Omega_H^2}}, \quad \text{(A.6)}$$

$$\Upsilon^{U}_{1L/R}(x) = f^{U,-}_{L/R}\frac{J(x)\Gamma_{L/R}(x)}{\sqrt{J^2(x)+4\Omega_H^2}}, \quad \text{(A.7)}$$

$$\Upsilon_{2L/R}(x) = f^{-}_{L/R}\frac{\Omega_H\Gamma_{L/R}(x)}{\sqrt{J^2(x)+4\Omega_H^2}}, \quad \text{(A.8)}$$

$$\Upsilon^{U}_{2L/R}(x) = f^{U,-}_{L/R}\frac{\Omega_H\Gamma_{L/R}(x)}{\sqrt{J^2(x)+4\Omega_H^2}}, \quad \text{(A.9)}$$

with $f^{\pm}_{L/R}$, $f^{U,\pm}_{L/R}$ defined below Eq. (14).

1. L.Y. Gorelik, A. Isacsson, M.V. Voinova, B. Kasemo, R.I. Shekhter, and M. Jonson, *Phys. Rev. Lett.* **80**, 4526 (1998).
2. D. Fedorets, L.Y. Gorelik, R.I. Shekhter, and M. Jonson, *Europhys. Lett.* **58**, 99 (2002).
3. R.I. Shekhter, Y. Galperin, L.Y. Gorelik, A. Isacsson, and M. Jonson, *J. Phys.: Condens. Matter* **15**, R441 (2003).
4. A. Erbe, C. Weiss, W. Zwerger, and R.H. Blick, *Phys. Rev. Lett.* **87**, 096106 (2001).
5. D.R. Koenig and E.M. Weig, *Appl. Phys. Lett.* **101**, 213111 (2012).
6. F. Pistolesi, *Phys. Rev. B* **69**, 245409 (2004).
7. A.N. Pasupathy, R.C. Bialczak, J. Martinek, J.E. Grose, L.A.K. Donev, P.L. McEuen, and D.C. Ralph, *Science* **306**, 86 (2004).
8. L.Y. Gorelik, D. Fedorets, R.I. Shekhter, and M. Jonson, *New J. Phys.* **7**, 242 (2005).
9. S.I. Kulinich, L.Y. Gorelik, A.N. Kalinenko, I.V. Krive, R.I. Shekhter, Y.W. Park, and M. Jonson, *Phys. Rev. Lett.* **112**, 117206 (2014).
10. O.A. Ilinskaya, S.I. Kulinich, I.V. Krive, R.I. Shekhter, H.C. Park, and M. Jonson, *New J. Phys.* **20**, 063036 (2018).
11. O.A. Ilinskaya, D. Radic, H.C. Park, I.V. Krive, R.I. Shekhter, and M. Jonson, *Phys. Rev. B* **100**, 045408 (2019).
12. L.Y. Gorelik, A. Isacsson, Y.M. Galperin, R.I. Shekhter, and M. Jonson, *Nature* **411**, 454 (2001).
13. A.V. Parafilo, I.V. Krive, R.I. Shekhter, and M. Jonson, *Fiz. Nizk. Temp.* **38**, 348 (2012) [*Low Temp. Phys.* **38**, 273 (2012)].
14. R.I. Shekhter, A. Pulkin, and M. Jonson, *Phys. Rev. B* **86**, 100404(R) (2012).

Вплив електрон-електронної взаємодії на термоіндуктоване шатлювання поляризованих за спіном електронів

О.О. Ільїнська, А.Д. Шкоп, D. Radic, H.C. Park, І.В. Кріве, R.I. Shekhter, M. Jonson

Розглядається одноелектронний транзистор з тепловим джерелом енергії, який складається з магнітних електродів і рухомого центрального острівця (квантової точки) і знаходиться в зовнішньому магнітному полі. Методом матриці густини вивчається можливість механічної нестійкості в цій системі, яка викликана магнітною обмінною взаємодією між поляризованими за спіном електронами. Аналітично доведено, що у випадку, коли електрони на квантовій точці не взаємодіють, такої механічної нестійкості немає. Для ненульової електрон-електронної взаємодії на квантовій точці чисельно знайдені критичні магнітні поля, що відокремлюють режим механічної нестійкості та електронного шатлювання від режиму механічних коливань, що загасають. Показано, що термоіндуктоване магнітне шатлювання поляризованих за спіном електронів — це порогове явище, і знайдено залежність порогової різниці температур від параметрів системи.

Ключові слова: термоіндуктований одноелектронний шатл, магнітна обмінна взаємодія, поляризовані за спіном електрони.

Влияние электрон-электронного взаимодействия на термоиндуцированное шаттлирование спин-поляризованных электронов

О.А. Ильинская, А.Д. Шкоп, D. Radic, H.C. Park, И.В. Криве, R.I. Shekhter, M. Jonson

Рассматривается одноэлектронный транзистор с тепловым источником энергии, состоящий из магнитных электродов и подвижного центрального островка (квантового дота), помещенный во внешнее магнитное поле. Методом матрицы плотности изучается возможность механической неустойчивости в этой системе, вызванной магнитным обменным взаимодействием между спин-поляризованными электронами. Аналитически доказано, что, если электроны на доте не взаимодействуют, такой механической неустойчивости нет. Для ненулевого электрон-электронного взаимодействия на доте численно найдены критические магнитные поля, отделяющие режим механической неустойчивости и электронного шаттлирования от режима затухающих механических колебаний. Показано, что термоиндуцированное магнитное шаттлирование спин-поляризованных электронов — это пороговый процесс, и найдена зависимость пороговой разности температур от параметров системы.

Ключевые слова: термоиндуцированный одноэлектронный шаттл, магнитное обменное взаимодействие, спин-поляризованные электроны.